Development 129, 1443-1453 (2002)
Printed in Great Britain © The Company of Biologists Limited 2002
DEV3535

Larval optic nerve and adult extra-retinal photoreceptors sequentially associate with clock neurons during *Drosophila* brain development

Sébastien Malpel, André Klarsfeld and François Rouyer*

Institut de Neurobiologie Alfred Fessard, CNRS UPR 2216 (NGI), 91198 Gif-sur-Yvette, France
*Author for correspondence (e-mail: rouyer@iaf.cnrs-gif.fr)

Accepted 12 December 2001

SUMMARY

The visual system is one of the input pathways for light into the circadian clock of the *Drosophila* brain. In particular, extra-retinal visual structures have been proposed to play a role in both larval and adult circadian photoreception. We have analyzed the interactions between extra-retinal structures of the visual system and the clock neurons during brain development. We first show that the larval optic nerve, or Bolwig nerve, already contacts clock cells (the lateral neurons) in the embryonic brain. Analysis of visual system-defective genotypes showed that the absence of the afferent Bolwig nerve resulted in a severe reduction of the lateral neurons dendritic arborization, and that the inhibition of nerve activity induced alterations of the dendritic morphology. During wild-type development, the loss of a functional Bolwig nerve in the early pupa was also accompanied by remodeling of the arborization of the lateral neurons. Approximately 1.5 days later, visual fibers that came from the Hofbauer-Buchner eyelet, a putative photoreceptive organ for the adult circadian clock, were seen contacting the lateral neurons. Both types of extra-retinal photoreceptors expressed rhodopsins RH5 and RH6, as well as the *norpA*-encoded phospholipase C. These data strongly suggest a role for RH5 and RH6, as well as NORPA, signaling in both larval and adult extra-retinal circadian photoreception. The Hofbauer-Buchner eyelet therefore does not appear to account for the previously described *norpA*-independent light input to the adult clock. This supports the existence of yet uncharacterized photoreceptive structures in *Drosophila*.

Key words: Bolwig organ, Hofbauer-Buchner eyelet, Circadian clock, Rhodopsins, *norpA*, Dendritic tree

INTRODUCTION

Most living organisms possess an endogenous circadian clock that runs, in constant conditions, with a species-specific period of ~24 hours. Environmental day-night cycles entrain the endogenous clock to a 24-hour period, or, stated otherwise, set the phase of the clock daily to solar time. Although phase shifts can be elicited by different stimuli, including temperature changes, light is by far the strongest entraining cue. In *Drosophila*, light-entrainable circadian clocks are scattered through numerous tissues (Plautz et al., 1997), but several lines of evidence indicate that a small group of neurons in the lateral brain is responsible for the control of locomotor activity and eclosion rhythms (Blanchardon et al., 2001; Helfrich-Förster, 1998; Renn et al., 1999). These so-called ventral lateral neurons (LN_vs) comprise two subsets of cells that express the products of the *period* (*per*) and *timeless* (*tim*) genes and synthesize the PDF (pigment-dispersing factor) neuropeptide, the main circadian neurotransmitter (Renn et al., 1999). Four small cell bodies (s-LN_vs) express PDF from the beginning of larval life through to the adult stage (Helfrich-Förster, 1997). During metamorphosis, PDF begins to be expressed in four to six large cells (l-LN_vs) that extensively arborize in the medulla and send contralateral projections through the posterior optic tract (POT) (Helfrich-Förster, 1997).

How do the *Drosophila* brain clock neurons see light? In contrast to mammals, whose eyes provide the only photic input to the clock located deep in the suprachiasmatic nucleus of the brain (Morin, 1994), flies appear to use several pathways for the light-resetting of their brain clock. The circadian clock of eyeless [e.g. *glass* (*gl*) or *sine oculis* (*so*)] or functionally blind [e.g. *no receptor potential A* (*norpA*) or *transient receptor potential* (*trp*)] mutants responds to light with a reduced sensitivity (Emery et al., 2000; Helfrich-Förster et al., 2001; Stanewsky et al., 1998; Wheeler et al., 1993; Yang et al., 1998). This suggests that the visual system contributes to circadian photoreception but that other components are involved as well. The finding of a *Drosophila* gene (*cry*) encoding a blue light photoreceptor, cryptochrome, has revealed a new clock-specific photoreception pathway (Emery et al., 1998; Stanewsky et al., 1998). cry^b mutants display defects in several clock responses to light (Stanewsky et al., 1998) that can be rescued by targeted CRY expression in the LN_vs, suggesting CRY-mediated light perception within the clock neurons themselves (Emery et al., 2000). As expected, $norpA^{P41}$; cry^b double mutants were more affected than either simple mutants in their entrainment to light-dark (LD) cycles (Emery et al., 2000; Stanewsky et al., 1998). However, the double mutants still entrained, indicating that a third input pathway is used by the brain clock to perceive light in a *norpA*-independent

manner (Hall, 2000; Stanewsky et al., 1998). This pathway appears to be *glass* dependent, as the clock that governs activity rhythms is completely blind in gl^{60J} cry^{b} double mutants (Helfrich-Forster et al., 2001); it may rely on the Hofbauer-Buchner (HB) eyelet, a set of extra-retinal neurons that project into the anterior medulla of the adult brain, where the LN_vs are located (Hall, 2000; Helfrich-Forster et al., 2001; Hofbauer and Buchner, 1989; Yasuyama and Meinertzhagen, 1999).

Although no clock-controlled behaviors have been characterized in larvae, larval clock function has been demonstrated by both molecular and behavioral studies (Kaneko et al., 2000; Kaneko et al., 1997; Sehgal et al., 1992). Sehgal et al. showed that the locomotor activity rhythm of the adults could be phased by a single 12-hour light episode during the first larval stage (Sehgal et al., 1992). In another study, short light pulses given to entrained third-instar larvae were shown to shift the phase of the molecular rhythms of the larval LNs and of the adult activity rhythms (Kaneko et al., 2000). Importantly, $norpA^{p41}$; cry^{b} double mutants were unable to entrain the molecular rhythms of their LNs to LD cycles delivered up to the third larval stage, suggesting that the larval light input pathways may be less redundant than in the adult, with a *norpA*-dependent visual system playing a more significant role (Kaneko et al., 2000). The larval visual system consists of a pair of 12-cells organs, the Bolwig organs (BO). These organs express chaoptin, as retinal photoreceptors do, and send axonal projections (the Bolwig nerves or BNs) that enter into the brain via the optic stalks as early as embryonic stage 16 (Green et al., 1993; Meinertzhagen and Hanson, 1993). The BO has been shown to mediate several light-induced larval behaviors (Busto et al., 1999; Hassan et al., 2000). In contrast to the retinal photoreceptors, the larval ones are cholinergic rather than histaminergic (Yasuyama et al., 1995), but seem to involve the same phototransduction cascade that uses rhodopsin(s) and *norpA*-encoded phospholipase C (PLC), according to the behavioral analysis of mutants (Busto et al., 1999; Hassan et al., 2000). Although their projections in the brain have not been extensively studied, they have been shown to terminate at the vicinity of the LNs, suggesting that the clock cells could be their direct targets (Kaneko et al., 1997).

We report strong developmental interactions between the BN and the LNs, which start very early during development. In addition, we show that the disappearance of the chaoptin-expressing BN at the beginning of metamorphosis coincides with a remodeling of the LNs, and is followed within ~1.5 days by the appearance of a new visual input to the LNs that comes from the neurons of the Hofbauer-Buchner eyelet underneath the retina. Interestingly, the photoreceptors of the adult eyelet and those of the Bolwig organ appear to express the same subset of rhodopsins, as well as the *norpA*-encoded PLC. The consequences of these findings for circadian photoreception are discussed.

MATERIALS AND METHODS

Strains and fly rearing

The visual mutant lines were *w*; gl^{60J} (Moses et al., 1989), *w* $norpA^{p24}$ (Pearn et al., 1996), *w*; eya^{2} (Pignoni et al., 1997), so^{1} (Cheyette et al., 1994) and so^{mda} (Serikaku and O'Tousa, 1994). Gene expression was driven in larval and adult photoreceptors by using the *w*; GMR-*hid* line (Bergmann et al., 1998) or in specific subsets of photoreceptors by using lines that carry rhodopsin promoter constructs *w*; *rh1-norpA* (McKay et al., 1995), *w*; *rh5-gfp* and *w*; *rh6-gfp* (Pichaud and Desplan, 2001), and *w*; *rh5-lacZ* and *w*; *rh6-lacZ* (Papatsenko et al., 2001). GMR (GLASS multimer reporter) constructs are expressed under the control of the GLASS transcription factor (as is the *chaoptin* gene) and therefore drive gene expression in all known photoreceptors. GAL4/UAS-controlled gene expression was used with the GAL4 enhancer-trap line *w*; *gal1118* (Blanchardon et al., 2001) and the *w*; *pdf-gal4* line (Park et al., 2000) for the LNs, the *w*; GMR-*gal4*/CyO line (Hay et al., 1994) for all photoreceptors, and the *w*; *rh1-gal4* (Hardie et al., 2001), *w*; *rh3-gal4*, *w*; *rh4-gal4* and *w*; *rh5-gal4* (Pichaud and Desplan, 2001) lines for specific photoreceptors. The UAS constructs carrying lines were *w*; UAS-*lacZ*, *w*; UAS-*gfp*, UAS-*cd8-gfp* (Lee and Luo, 1999), *w* UAS-*hid* UAS-*rpr* (Zhou et al., 1997) and *yw*; UAS-*Kir2.1* (Baines et al., 2001). The *gal1118* on the third and UAS-*gfp* insertion on the second chromosome were transferred into the *w*; gl^{60j} and the *w*; eya^{2} backgrounds by standard crosses. As *norpA* is on the X chromosome, *gal1118*-driven GFP staining in the $norpA^{p24}$ background was obtained by dissecting male larvae from crosses between female $norpA^{p24}$ and male *w*; UAS-*gfp*; *gal1118* flies. In that case, the female larvae were used as controls. *w*; UAS-*gfp*; *gal1118* flies were also used for crosses with GMR-*hid* flies. *Drosophila* cultures were usually maintained on a 12 hours/12 hours dark/light cycle on standard corn meal-yeast-agar medium at 25°C and 50% relative humidity. For some experiments, flies were kept in permanent darkness. Closely synchronized pupae were obtained by transferring white prepupae to fresh bottles. This was considered as time zero after puparium formation (APF). GMR-*gal4*-driven KIR 2.1 expression caused some lethality, as judged from the number of eclosed flies with the CyO balancer chromosome rather than the GMR-*gal4* one. This was also observed when expressing other deleterious proteins under GMR control (Kitamoto, 2001). Lethality at 25°C was 80±2% (n=3 experiments with 80-110 flies counted in each). In one experiment performed at 19°C, lethality was 60% (162 flies counted).

Histology

Central nervous systems from third instar larvae, staged pupae and adults were dissected as described elsewhere (Blanchardon et al., 2001), except that primary antibody incubations were shortened to 4 hours at room temperature or overnight at 4°C, and the samples were preincubated with 10% normal goat serum before secondary antibody labeling. Embryos were dechorionated for 5 minutes with bleach on a plastic filter, rinsed and prefixed in an Eppendorf vial containing a 1:1 mix of heptane and 4% paraformaldehyde in phosphate-buffered saline (PBS). After the vial was turned slowly for 15 minutes, the lower (aqueous) phase was eliminated with a Pasteur pipette, and the embryos were collected in a small volume of heptane. They were forced on to a double-faced Scotch tape on the bottom of a small hollow dissection chamber filled with 4% paraformaldehyde in PBS, and the vitelline membrane was removed manually under a stereomicroscope. The embryos were then rinsed several times with PBS before proceeding with the standard immunofluorescence protocol (except that primary antibody concentrations were doubled). GFP was clearly visualized on live, dechorionated embryos, but it was lost during their further immunocytochemical processing. *gal1118*-driven UAS-*lacZ* expression was therefore used to detect the LNs in embryos. It was revealed with either a monoclonal anti-β-galactosidase antibody or a rabbit anti-β-galactosidase antiserum (for double-labeling experiments with mAb 24B10), which resulted in a higher background. Dilutions for the antibodies were as follows: mouse anti-chaoptin monoclonal antibody (mAb 24B10) (Fujita et al., 1982), 1/100; mouse anti-ChAT monoclonal antibody (mAb 4B1) (Yasuyama et al., 1995), 1/100; mouse anti-β-galactosidase monoclonal antibody (Promega), 1/1000; rabbit anti-crab β-PDF

(Dircksen et al., 1987), 1/5000; rabbit anti-NORPA (Zhu et al., 1993), 1/5000; and rabbit anti-β-galactosidase polyclonal antibody (gift from B. Limbourg-Bouchon), 1/100. Labeling of the *so*^{mda} and GMR-*gal4*/+; UAS-*Kir 2.1*/+ brains and their corresponding controls was performed with a newly generated rabbit anti-*Drosophila*-PDF (Neosystem, Strasbourg, France) with high specificity and low background, at 1/10000 dilution. Secondary antibodies were Texas Red or Alexa594-conjugated goat antibodies to rabbit IgG (Cappel or Molecular Probes, respectively), Texas Red- or Cy2-conjugated goat antibodies to mouse Ig (Cappel or Amersham, respectively). They were used at 1/1000 dilution, except for the Alexa594-conjugated goat antibodies (1/10000).

Imaging and image analysis

For measurements of the dendritic arborization of LNs, each mutant genotype was tested independently, in parallel with an identically treated wild-type control. Images were made from an epifluorescence microscope (Zeiss Axioplan2) with a cooled digital camera (Diagnostic Instruments SPOT2). For every half brain, the presence or absence of a GFP-stained dendritic arborization was scored (see Table 2). When it was present, its area in pixels was measured on the image, using a specific function of the SPOT2 software. The average area for a given genotype was normalized to that of the wild-type control in the same experiment, allowing comparison between the mutant strains. Confocal imaging was performed with a Leica TCS4D or SP2 confocal microscope.

RESULTS

Anatomical evidence for a cholinergic contact between BN and the larval LNs

The BN is known to end close to the LNs in the brain of third instar larvae (Kaneko et al., 1997). We first asked whether the BN actually contacts the clock cells. Double staining, using the visual system-specific GMR-*gal4* or anti-chaoptin antibody, and PDF immunoreactivity, indicated a close interaction between the BN ending and the dendritic arborization of the LNs in third-instar larval brains (Fig. 1A-C,G). Because the BN has been shown to be cholinergic (Yasuyama et al., 1995), double labeling was achieved with an anti-choline-acetyltransferase (ChAT) antibody and GFP-expression driven by the *gal1118* enhancer trap that is strongly expressed in the LNs (Blanchardon et al., 2001). The axon terminals of the BN that contact the dendritic arborization of the LNs indeed contained the acetylcholine-synthesizing enzyme ChAT (Fig. 1H), suggesting further that transmission between the two structures is acetylcholine mediated. Regarding the upstream signaling cascade, we also observed that the *norpA*-encoded PLC is expressed in the BN fibers that interact with the LNs (Fig. 1I). We then asked which rhodopsins would be expressed in the BN fibers that contact the LNs. *rh5* (Fig. 1D) and *rh6* (Fig. 1E) genes were seen to be expressed in the BO, whereas the *rh1* gene (which encodes the main retinal rhodopsin) was not (data not shown). *rh5*- and *rh6*-expressing fibers seemed to contact the LNs to the same extent, at least at this level of analysis. They formed two non-overlapping subsets of the BN fibers (Fig. 1F). These results suggest that RH5, RH6 and NORPA are components of circadian photoreception in larvae.

The contact between the BN and the LNs occurs during embryogenesis

In order to determine when the BN contacts the LNs during brain development, double staining experiments were performed at earlier developmental stages. PDF expression is first detected in the LNs at about 6 hours into the first larval

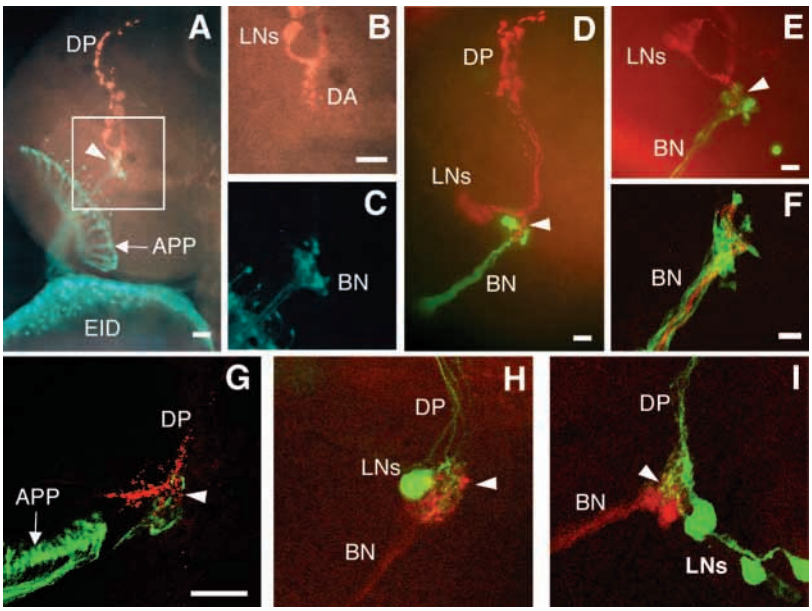

Fig. 1. Anatomical contact between the Bolwig nerve and the lateral neurons in wild-type third instar larvae. (A-C) Whole-mounted CNS of a third instar *w*; GMR-*gal4*/UAS-*gfp* larva, with one eye imaginal disc (epifluorescent microscopy). The white box indicates the region shown in greater detail in B and C. Green (A,C): staining of the visual system with GMR-*gal4*-driven GFP expression. Red (A,B): anti-β-PDF staining of the lateral neurons. (D,E) Whole-mount of third instar larval CNS (epifluorescent microscopy). The LNs are visualized by anti-β-PDF antibody (red). Expression of the rhodopsin genes in the Bolwig organ is detected through reporters driven by specific promoters. (D) Green: GFP staining of the BN in a *w*; UAS-*gfp*/+; *rh5-gal 4*/+ larva. (E) Green: β-galactosidase expression in the BN revealed by anti-β-gal antibody in a *w*; *rh6-lacZ* larva. (F) Confocal reconstruction. Double staining of the BN in a *w*; *rh6-gfp*/*rh5-lacZ* larva shows that *rh5* and *rh6* are expressed in different axons (and therefore different cells) of the BN. Green, GFP staining of *rh6*-expressing fibers; red, anti- β-gal staining of *rh5*-expressing fibers. No *rh1* expression was found in the BN using either *rh1-gal4* (with a UAS-*gfp* reporter) or *rh1-norpA* (with anti-NORPA antibody) constructs. (G-I) Whole-mounts of third instar larval CNS (confocal microscopy) (G,H, 1 μm single optical section; I, five projected optical sections). (G) Anti- β-PDF staining (red) reveals the LNs and anti-chaoptin staining (green) reveals the BN in a wild-type larva (*w*). Like the GMR-*gal4* transgene used in A-C, the *chaoptin* gene is expressed in both larval and adult photoreceptors. (H,I) LNs are visualized by GFP expression (green) in *w*; UAS-*gfp*; *gal1118* larvae. Anti-ChAT (H) or anti-NORPA (I) immunoreactivities (red) label the BN. No anti-NORPA labeling was observed in the BN of *norpA*^{P24} mutant larvae (not shown). APP, adult photoreceptors projections; BN, Bolwig nerve; DA, dendritic arborization of LNs; DP, dorsal projections of LNs; EID, eye-antenna imaginal disc; LNs, lateral neurons. Arrowheads indicate contact between BN terminus and LNs dendritic arborization. Scale bars: 10 μm.

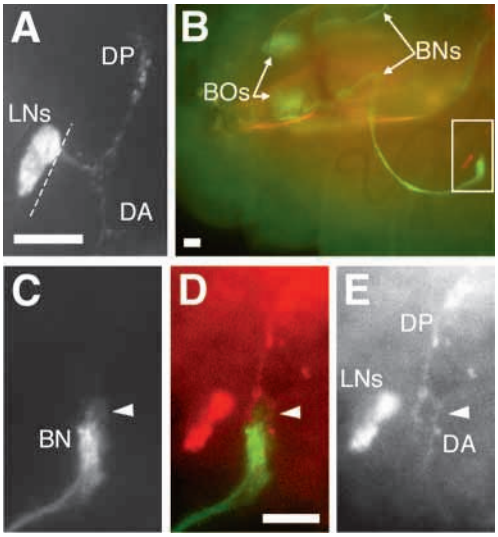

Fig. 2. Anatomical contact between the Bolwig nerve and the lateral neurons in wild type embryo. (A) Whole-mount of a stage-17 *w*; UAS-*lacZ*; *gal1118* embryo stained with a monoclonal anti-β-gal antibody to detect the LNs (see Materials and Methods). Broken line indicates the limit between different focal planes. Neurites extending from the labeled cells were seen in 10 out of 17 hemispheres. (B-E) Whole-mount of a stage-17 *w*; UAS-*lacZ*; *gal1118* embryo double-stained with a polyclonal anti-β-gal antibody and the anti-chaoptin antibody to reveal the visual system. We also found embryos with only the BO/BN labeled and no detectable *gal1118* expression in the LNs (data not shown). This is consistent with the start of *gal1118* expression at the beginning of stage 17 that we observed with *gal1118*-driven GFP in live embryos (not shown). (B) The two Bolwig organs are visible near the oral armature and their projections run around the CNS towards their targets. (C-E) detail of the contact zone (white box in B) from the same embryo at higher magnification. [C,D (green)] Anti-chaoptin staining of the BN termination. [D (red), E] Anti-β-gal staining of the LNs and their projections. The BN ending appeared to contact the smaller one of the two main neuritic branches, which presumably represents an early stage of development of the dendritic arborization illustrated in Fig. 1. BN, Bolwig nerve; BOs, Bolwig organs; DA, dendritic arborization of LNs; DP, dorsal projections of LNs; LNs, lateral neurons. Arrowheads indicate the contact zone. Scale bars: 10 μm.

stage (Helfrich-Förster, 1997), and a contact between the BN and the LNs was observed at that stage (not shown). However, the BN ends its extension into the central brain around late embryonic stage 16 (Green et al., 1993). Using *gal1118* expression, the LNs were first detected in stage-17 embryos (Fig. 2A), with an average of 3.1±0.2 cells per brain hemisphere (n=15). Contact between the dendritic processes of the LNs and the BN was already observed at that stage (Fig. 2B-E).

The BN is required for the development or the maintenance of the dendritic arborization of the larval LNs

To test whether the BN and the LNs influence each other's differentiation, we looked for defects in either one of the two structures when the other was deleted. The morphology of the BN terminal was analyzed in larvae whose LNs were ablated as a consequence of the simultaneous expression of both *head-*

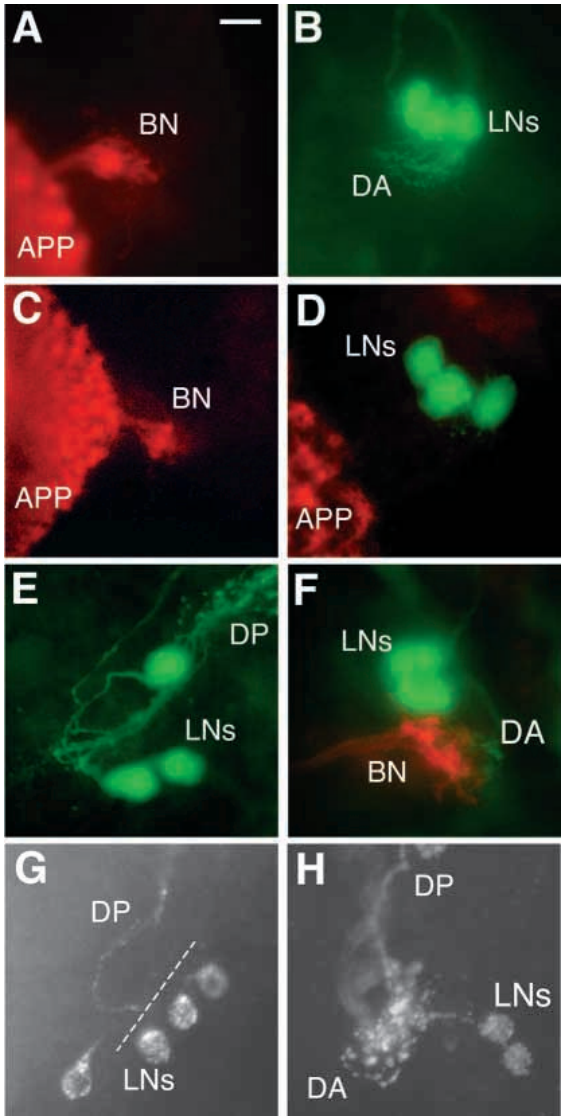

Fig. 3. Atrophy of the dendritic arborization of the lateral neurons in the absence of the BN. (A-F) Whole-mounts of third instar larval CNS; LNs are stained with GFP (green) and the visual system with anti-chaoptin (red). (A,B) Visual system (A) and LNs (B) in a *w*; UAS-*gfp*/+; *gal1118*/+ control CNS. (C) Apparently normal visual system in a *w* UAS-*hid* UAS-*rpr*/*w*; UAS-*gfp*/+; *gal1118*/+ CNS (as observed in 10 out of 10 brains). (D) BN-depleted visual system and LNs without dendritic arborization in a *w*; GMR-*hid*/UAS-*gfp*; *gal1118*/+ CNS. Although the BN was always undetectable in these third instar larval brains, the developing adult photoreceptors were present. They only degenerated during pupal life (data not shown), presumably when the apoptotic pathways were fully activated by HID expression. (E) Absence of visual system, and LNs without any detectable dendritic arborization in a *w*; UAS-*gfp*/+; gl^{60J} *gal1118*/ gl^{60J} CNS. (F) Visual system without adult photoreceptors and LNs with their dendritic arborization in a *w*; eya^{2} UAS-*gfp*/ eya^{2}; *gal1118*/+ mutant. (G,H) Whole-mounts of third instar larval CNS. LNs are stained with anti-PDF. (G) LNs without dendritic tree in a so^{mda} mutant. Broken line indicates the limit between different focal planes. (H) Wild-type LNs. A dendritic arborization was observed in only 9% of so^{mda} brain hemispheres (n=34), versus 92% of controls (n=13). APP, adult photoreceptors projections; BN, Bolwig nerve; DA, dendritic arborization of LNs; DP, dorsal projections of LNs; LNs, lateral neurons. Scale bar: 10 μm.

Table 1. Quantitative comparison of the dendritic arborization area of the third instar larvae LNs

Genotype	Percentage of half-brains with detectable dendritic arborization (*n*)	Relative average area of the dendritic arborizations (±s.e.m.)	Total number of half-brains
w	91% (78)	100 (±4)	86
gl^{60J}	18% (3)	35 (±9)	17
GMR-hid	28% (5)	41 (±8)	18
eya^{2}	94% (15)	129 (±12)	16
$norpA^{p24}$	92% (37)	97 (±5)	40
w DD	86% (18)	109 (±10)	21

Average area of the wild-type arborization was about 180 μm^2.

involution defective (*hid*) and *reaper* (*rpr*) pro-apoptotic genes under *gal1118* control. No obvious defect was observed in the BN axonal projections in third-instar larval brains (Fig. 3, compare C with A), although the LNs were completely absent. To analyze the effect of BN ablation on the LNs, we used the GMR-*hid* line, which expresses the *hid* gene in the visual system. A complete ablation of the BN was observed and the dendritic tree of the LNs was extremely reduced, down to totally undetectable in the majority of *w*; GMR-*hid*/UAS-*gfp*; *gal1118*/+ larval brains (Table 1) as illustrated in Fig. 3 (compare D with B).

In order to determine whether the lack of BN is necessary and sufficient to cause the reduction of the LNs dendritic arborization, we measured the latter in several visual system mutants. The gl^{60J} mutation prevents all photoreceptor differentiation, resulting in the lack of a functional BN (Moses and Rubin, 1991). In gl^{60J} brains, the LNs showed a phenotype very similar to the one caused by GMR-*hid*, namely a total absence of their dendritic arborization in a large majority of brains and a size reduction in the minority of the brains with detectable arborization (Table 1), as illustrated in Fig. 3E. Similar results were obtained with the so^{mda} allele of the *sine oculis* gene (Fig. 3, compare G with H), in which the larval photoreceptors fail to differentiate and the adult photoreceptors cannot innervate the brain (Serikaku and O'Tousa, 1994).

The *eyes absent*^{2} (eya^{2}) mutation results in the absence of any adult photoreceptors (Bonini et al., 1993) without affecting the BN, which was thus the only visual structure stained in late third-instar larval brains (Fig. 3F). This situation is the opposite to that found for GMR-*hid* (see Fig. 3D), namely the absence of the BN and the presence of developing adult photoreceptors reaching into the brain. Contrary to GMR-*hid*, gl^{60J} or so^{mda}, the dendritic arborization of the LNs in eya^{2} larvae appeared normal (Fig. 3F and Table 1), thus further confirming that the BN is specifically required for the presence of a wild-type dendritic arborization of the LNs.

Light-dependent BN activity is not required for normal morphological differentiation of the larval LNs

In an attempt to define how the larval optic nerve affects the dendritic arborization of its target LNs, we examined the role of light-driven BN activity by analyzing blind or dark-reared flies. The null $norpA^{p24}$ mutation blocks the phototransduction cascade in the adult photoreceptors, and is likely to do so in the BN (Busto et al., 1999; Hassan et al., 2000). The dendritic arborization of the LNs was of normal size in this mutant as it was in wild-type larvae reared in complete darkness throughout development (*w* DD, Table 1). These results show that the development of the dendritic tree of the LNs does not depend on the phototransduction cascade within the BN.

In order to test whether some light-independent activity of the BN might be involved, we expressed under GMR-*gal4* control several molecules expected to alter or block BN function and analyzed their effect on the LNs. Tetanus-toxin light chain expression in the BN did not appear to affect the morphology of either the BN or the LNs (data not shown). However, expression of a potassium channel (KIR2.1) known to hyperpolarize neurons and strongly inhibit the firing of action potentials (Baines et al., 2001) led to alterations of both the nerve and its target arborization (Fig. 4A,B). These results suggest that light-independent activity of the BN is necessary and sufficient to induce and maintain the normal morphology of the dendritic arborization of the LNs. Interestingly, similar LNs defects were observed in a fraction of wild-type brains at the beginning of metamorphosis (Fig. 4C,D), when the BN might have begun to lose activity before it becomes undetectable with photoreceptor-specific markers.

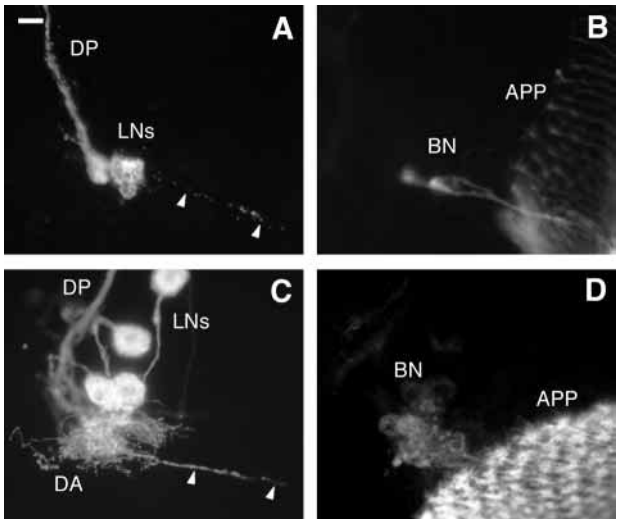

Fig. 4. Extension of dendritic arborization of the larval LNs, caused by Kir2.1 expression in the visual system, and in a wild-type prepupa. (A,B) Whole-mount of a doubly stained CNS of *w*; GMR-*gal4* UAS-*gfp*/+; UAS-*Kir2.1*/+ third instar larval brain. (A) Anti-PDF staining of the LNs. Arrowheads indicate the long PDF-immunoreactive extension (seen in 9/10 hemispheres, versus 0/6 for the third instar controls in the same experiment, not shown). Similar alterations were already detectable in the first larval stage (not shown). (B) GFP staining of the visual system. The BN ending is much thinner than normal (compare with Fig. 1C). (C,D) Whole-mount of a doubly stained CNS of control *w*; UAS-*cd8-gfp*; *gal1118* at 4 hours after puparium formation (APF). CD8-GFP is used instead of GFP to label the processes of the LNs better. (C) CD8-GFP staining of LNs. The same kind of extension has been seen in about 10% of hemispheres from three independent experiments (also with *pdf-gal4* driven UAS-*gfp* expression in the LNs) performed within approximately 6 hours around puparium formation. (D) Anti-chaoptin staining of the visual system. No morphological alterations were observed. APP, adult photoreceptors projections; BN, Bolwig nerve; DA, dendritic arborization of LNs; DP, dorsal projections of LNs; LNs, lateral neurons. Scale bar: 10 μm.

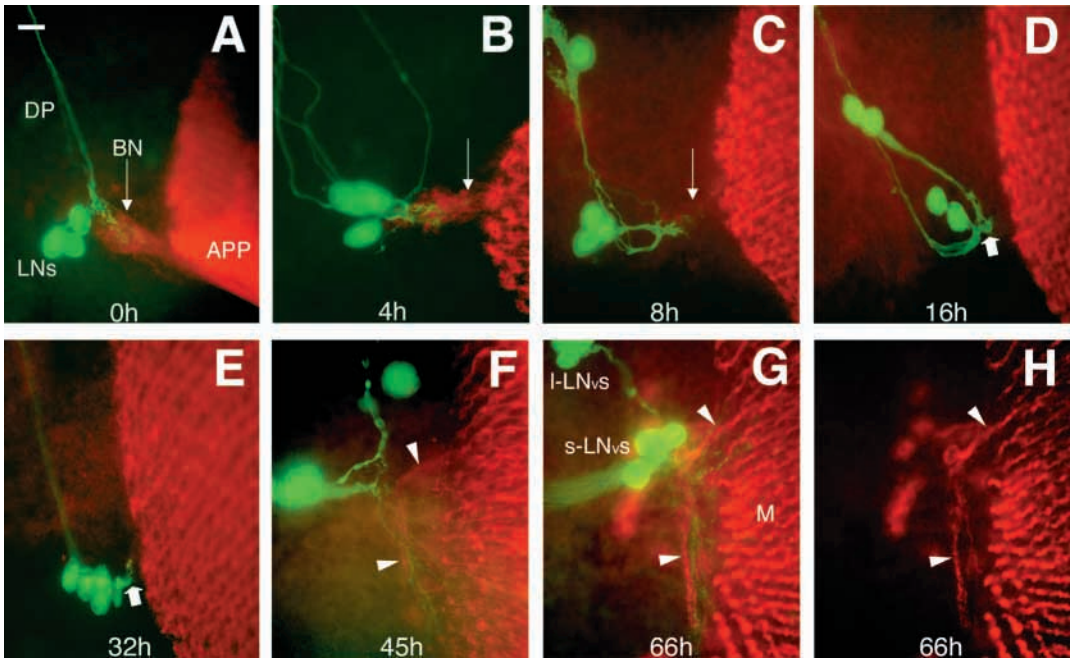

Fig. 5. Changes in the visual system and the LNs during pupation. Whole mounts of *w*; *pdf-gal4* UAS-*gfp* pupal brains doubly stained with anti-chaoptin (red) for the visual system and GFP (green) for the LN_vs. Similar results were obtained with both *gal1118*-driven GFP labeling and anti-PDF labeling of the LN_vs (not shown). However, most of the experiments were performed with *pdf-gal4*-driven GFP labeling, because it remained restricted to the s-LN_vs for the longest developmental time, thus ensuring that the arborization observed up to 32 hours APF indeed originated from the s-LN_vs and not from the l-LN_vs. Time APF is indicated in hours. Thin arrows indicate the BN that is detected up to 8 hours APF (A-C). (D,E) Thick arrows indicate the reduced dendritic arborization of the LNs at 16 hours (D) and 32 hours (E) APF. Arrowheads show the newly appeared chaoptin-expressing fiber (F-H). G,H are the same sample, but H shows only chaoptin staining for better visualization. APP, adult photoreceptors projections; BN, Bolwig nerve; LNs, lateral neurons; DP, dorsal projections of LNs; l-LN_vs, large ventral lateral neurons; s-LN_vs, small ventral lateral neurons; M, medulla. Scale bar: 10 μm.

The disappearance of the BN terminal after pupariation is accompanied by rapid changes in the morphology of the dendritic arborization of the LNs and followed by the appearance of new photoreceptive afferents

The BN has been reported to disappear soon after the onset of pupariation (Tix et al., 1989). In our hands, complete disappearance of BN as inferred from chaoptin staining occurred between 8 and 16 hours APF at 25°C (Fig. 5C,D). In parallel, we noticed a 2.5- to 3-fold reduction of the LNs dendritic arborization (Fig. 5, compare A-C with D,E; quantified in Fig. 6). Between 16 and 32 hours APF, no photoreceptor afferent of the LNs could be detected with anti-chaoptin labeling, as illustrated in Fig. 5D,E. However chaoptin-expressing fibers, which extended beyond the medulla towards the LNs, were detected again at 45 hours APF and persisted into the adult stage (Fig. 5F-H and Table 2). Their appearance was synchronous with that of an arborization of the LNs of much wider size than the larval one (Fig. 5F,G and Table 2). This arborization seemed to originate from the l-LN_vs, which start expressing PDF at mid-pupation (Helfrich-Förster, 1997).

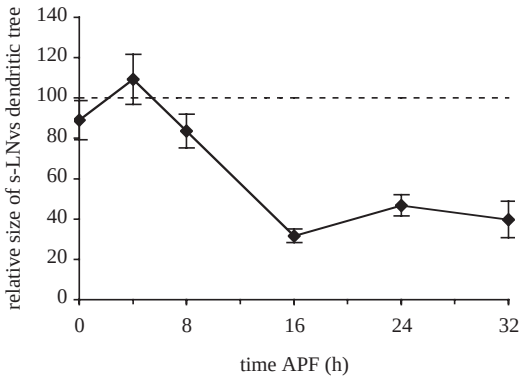

Fig. 6. The dendritic arborization of the s-LN_vs regresses during early metamorphosis. The ordinate shows the average relative size of the dendritic arborization of the LNs where 100 is the mean value for the L3 larvae used as reference. The *x*-axis indicates time spent APF. Bars indicate s.e.m. Quantification was performed on GFP labeling in s-LN_vs of *w*; *pdf-gal4* UAS-*gfp* at times when GFP expression could not yet be detected in the l-LN_vs (see also legend to Fig. 5).

The adult chaoptin-expressing fibers contacting the LN_vs from mid-metamorphosis come from the Hofbauer-Buchner eyelet

The chaoptin-expressing fibers that appear at mid-pupation (Fig. 5F-H) have many characteristic features of previously described visual fibers originating from the so-called Hofbauer-Buchner eyelet, and extending into the anterior medulla (Hofbauer and Buchner, 1989).

(1) The eyelet expresses a specific rhodopsin isoform, RH6 (Yasuyama and Meinertzhagen, 1999). Similarly, we found that the *rh6-gfp* construct strongly labeled the LN_vs-contacting

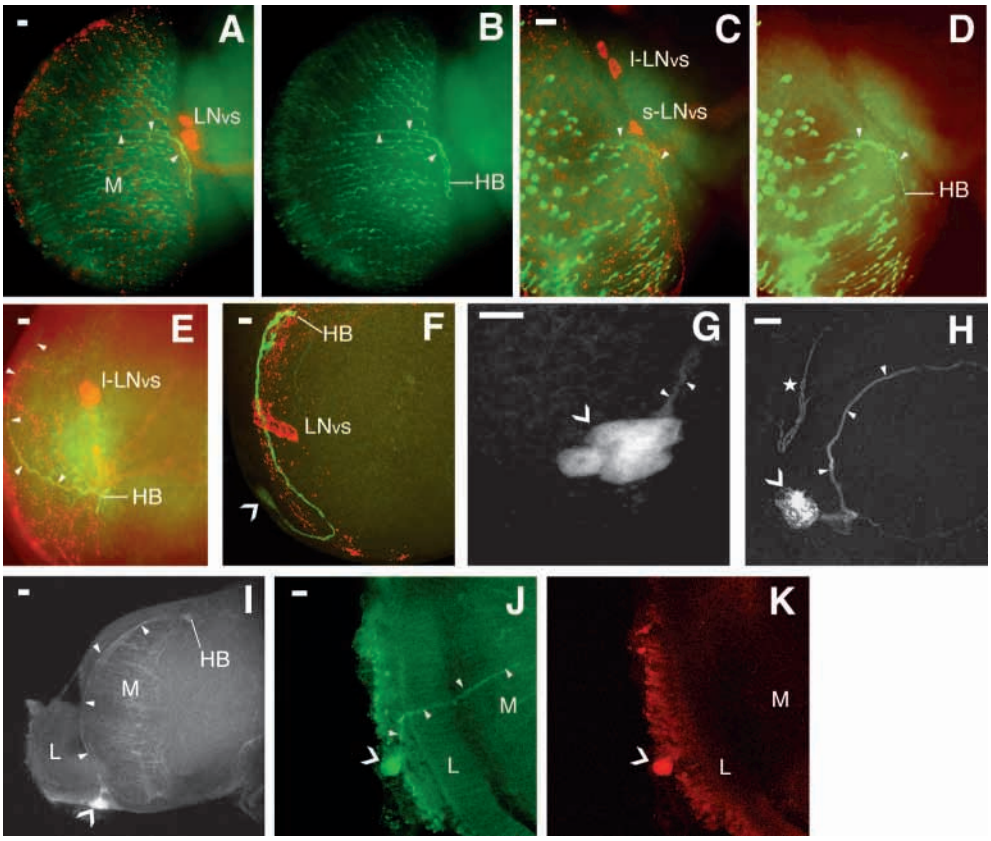

Fig. 7. The HB eyelet contacts the LN_vs in wild type and *so*^{1} mutants, and expresses *rh5*, *rh6* and the *norpA* gene product. (A-D) Whole mount of wild-type adult brains in epifluorescent microscopy. (A) Double staining of retinal R8 and eyelet projections with GFP (green) and of the LN_vs with anti-PDF (red) in a *w*; *rh6-gfp/+* brain. (B) The same brain with GFP staining only. (C) Double staining of retinal R8 and eyelet projections with GFP (green) and anti-PDF (red) in a *w*; UAS-*gfp*/+; *rh5-gal4*/+ brain. (D) The same brain with GFP staining only. Staining of LN_vs-contacting fibers has been detected in 6 out of 26 hemispheres. No such staining was observed with either *rh5-lacZ* or *rh5-gfp* constructs (not shown). As a control for *rh5-gal4* and *rh6-gfp* expression, staining of retinal photoreceptors projections [~70% of R8 fibers for *rh6-gfp* and 30%, for *rh5-gal4* (Pichaud et al., 1999)] indicated that both constructions were specifically expressed in these cells. (E-G) Whole-mount of mutant *w; so*^{1} *rh6-gfp*/*so*^{1} late pupal brains. Pupal brains were used here because their HB eyelet somata remained attached to the optic lobes more frequently than in adult brains. (E,F) HB eyelet is labeled with *rh6*-driven GFP (green) and LN_vs are labeled with anti-PDF (red). (E) Whole mount brain in epifluorescent microscopy. (F) Confocal projection of another sample shows the whole pathway of the HB fiber, from the somata outside of the PDF-labeled arborization in the medulla, to its target area inside the brain. (G) *rh6*-driven GFP expression in the HB somata of another sample at higher magnification (confocal projection). (H) Presence of the eyelet in the *so*^{mda} mutant. A *w*; *so*^{mda} mutant brain is stained with anti-chaoptin antibody, which reveals the eyelet cell bodies and projections (confocal projection). Such staining was observed in five out of 39 brain hemispheres, with clearly recognizable cell bodies in two of them. The space corresponding to the optic lobes was always filled with unorganized material (not shown). The star indicates an autofluorescent tracheal structure. (I-K) Expression of the *ro-tauZ* transgene in the eyelet of wild-type flies (whole mounted *w*; *ro-tauZ* adult brains, confocal projections). That construct drives *tau-lacZ* expression from an artificial promoter comprising *rough* and *Krüppel* enhancers (F. Pichaud and U. Gaul, personal communication). (I) Horizontal view of the HB pathway stained with anti-β-gal antibody. Stained fibers in the larger part of the medulla are from unknown origin. (J,K) Doubly stained brain with anti-β-gal (J, green) and anti-NORPA (K, red) antibodies. The *ro-tauZ* expressing eyelet is labeled by anti-NORPA. Similar results were obtained in *so*^{1} brains (not shown). No such staining was observed in a *norpA*^{P24} mutant context (not shown). The arrowheads indicate HB eyelet pathway. The V-shaped arrowheads indicate HB eyelet somata. HB, termination of the Hofbauer-Buchner eyelet; LN_vs, ventral lateral neurons; l-LN_vs, large ventral lateral neurons; s-LN_vs, small ventral lateral neurons; L, lamina; M, medulla;. Scale bars: 10 μm.

fibers in the adult brain (Fig. 7A,B). It allowed us to follow their long ventral course, alongside the PDF-expressing arborization, showing that the two structures had a much more extensive contact zone than could be deduced from sectioned material (Hofbauer and Buchner, 1989; Yasuyama and Meinertzhagen, 1999).

(2) The eyelet is preserved in the *so*^{1} mutant context, where the projections from the R1 to R8 photoreceptors are almost always absent (Hofbauer and Buchner, 1989). Similarly, we detected *rh6-gfp* expression in the LN_vs-contacting fibers in more than half of the *so*^{1} mutant brains, as illustrated in Fig. 7E-G. The absence of most other photoreceptors allowed us to

Table 2. Developmental timing of adult-specific visual fibers and ventral extension of the l-LN_vs arborization

	Time APF				
	32 hours	45 hours	66 hours	72 hours	96 hours
Average number of l-LN_vs somata	0	1.9 (±0.3)	3.3 (±0.2)	3.4 (±0.2)	3.3 (±0.2)
Ventral extension from l-LN_vs	0/8*	7/17†	16/16	16/16	17/17
Presence of the new visual fiber	0/8	5/14†	15/15	14/14	13/13

*Denominators represent the total number of brain hemispheres labeled at each time point.

†Absence or presence of both the ventral extension from the l-LN_vs and the new visual fiber could be reliably scored in 13 brain hemispheres: two out of 13 displayed only the ventral extension from l-LN_vs, one out of 13 only the visual fiber, four out of 13 displayed both, while six out of 13 displayed none. However, all brains displaying the new visual fiber had at least one detectable l-LN_v cell body.

follow the fibers back, sometimes all the way to the corresponding cell bodies. They could be discerned on the outside margin of the much-reduced *so*^{1} optic lobes, which lack a lamina (Fig. 7F,G). Interestingly, such cell bodies were also sometimes observed in the *so*^{mda} mutant context (Fig. 7H), although optic lobes were completely absent and no retinal axon entered the brain (not shown) (Serikaku and O'Tousa, 1994).

(3) The HB cell bodies are located beneath the posterior retina (Hofbauer and Buchner, 1989; Robinow and White, 1991; Yasuyama and Meinertzhagen, 1999) and project toward the anterior medulla (Hofbauer and Buchner, 1989). In order to visualize the LNs-contacting fibers together with the corresponding cell bodies in a wild-type context, we used a *ro-tauZ* construct that is co-expressed with *rh6-gfp* only in these fibers (data not shown). As expected for the eyelet, the *ro-tauZ*-labeled cell bodies were found immediately outside the distal margin of the lamina (Fig. 7I,J), with their fibers projecting to the anterior medulla (Fig. 7I), where they contacted the LN_vs (not shown).

Phototransduction components within the eyelet

We then asked whether the eyelet would express the same phototransduction components than those expressed in the BO, in addition to RH6. NORPA expression was indeed detected in the eyelet of wild-type (Fig. 7K) and *so*^{1} flies (not shown). Although no RH5 was detected with a specific antibody, as previously described (Yasuyama and Meinertzhagen, 1999), we observed a weak expression of *rh5-gal4* in the HB fibers (Fig. 7C,D), in 23% of dissected brain hemispheres. No labeling was seen with either *rh3-gal4* or *rh4-gal4* (not shown). These data indicate that the HB eyelet may use the same rhodopsins and phototransduction pathway as the BO.

DISCUSSION

In *Drosophila*, the PDF-expressing LNs control the circadian rhythmicity of both adult activity and eclosion (Blanchardon et al., 2001; Helfrich-Förster, 1998; Renn et al., 1999). A subset of the LNs is present in the larval brain (Helfrich-Förster, 1997) where they already express PER and TIM cyclically (Kaneko et al., 2000; Kaneko et al., 1997). We show that the LNs are connected to the BO during embryonic development and become the direct target of the Hofbauer-Buchner eyelet at mid-metamorphosis. In addition, our results strongly suggest that light input from these organs to the clock relies on the RH5 and RH6 rhodopsins, as well as on the *norpA*-encoded PLC.

Precocious interaction between the BN and clock neurons

Differentiation of the BO starts at stage 12, and includes a multi-step elongation of the BN that pauses near the superficial optic lobe pioneer cells (OLPs), and finally reaches its target(s) inside the central brain at stages 16-17 (Campos et al., 1995; Green et al., 1993; Schmucker et al., 1997). The *gal1118* enhancer-trap line (Blanchardon et al., 2001) shows that the LNs are already present at embryonic stage 17. Their differentiation had probably occurred even earlier, as neuritic processes were already observed at that stage. Taking into account the various time lags introduced by the GAL4/UAS system, actual *gal1118* expression in the LNs may similarly start as soon as or even before the BN reaches the central brain.

Use of *gal1118*-driven GFP fluorescence revealed that the dendritic tree of the LNs in third instar larvae is much larger than described with PDF immunocytochemistry and displays extensive intertwining with the BN ending. The presence of the acetylcholine-synthesizing enzyme ChAT in the terminal branches that contact the LNs strongly suggests that cholinergic synapses transmit light information from the BO to the clock cells, although additional transmitters are not excluded. Because the BN fasciculates with the axons of the OLPs (Campos et al., 1995), the latter may also contact the LNs. This possibility is strengthened by the fact that at least one of the OLPs is cholinergic (Yasuyama et al., 1995).

Larvae carrying the *norpA*^{p24} mutation show defects in some light-induced behaviors (Busto et al., 1999; Hassan et al., 2000), but the presence of the *norpA*-encoded PLC in the BO has not been documented before. Its detection down to the BN ending contrasts with the absence of detectable PLC immunoreactivity in the adult retinal axons (data not shown) (see also Fig. 7K) (McKay et al., 1995; Zhu et al., 1993). This different subcellular distribution could be due to the lack of specialized rhabdomeres in the BO cells (Green et al., 1993). It could also reflect the expression of different PLC isozymes by alternative splicing from the *norpA* locus (Kim et al., 1995; Zhu et al., 1993). Expression of the retinal subtype I transcripts would be expected in the BO, but only body subtype II transcripts were reported in pre-adult stages (Kim et al., 1995). Whether the subcellular targeting of the two PLC isozymes differs is not known. In any case, NORPA distribution all along the BN suggests that the relevant isozyme is involved in more than phototransduction.

This report indicates that the *rh5* and *rh6* genes are expressed in the BO but that *rh1* is not. Similar data, as well as the absence of *rh3* and *rh4* expression, have been recently cited as unpublished results (Papatsenko et al., 2001). Interestingly, some larval responses to light have been reported to rely on RH1 (Busto et al., 1999; Hassan et al., 2000), suggesting a role for RH1 outside the BO. In the adult eye, RH5 and RH6 are found in different sets of R8 photoreceptors (Chou et al., 1996; Huber et al., 1997; Papatsenko et al., 1997). Our data similarly suggest a mutually exclusive expression of the two types of rhodopsins in the larval photoreceptors, as RH5- and RH6-expressing fibers do not appear to overlap in the BN.

Visual afferences affect the differentiation of clock neurons

The ablation of the LNs did not induce morphological changes at the BN terminus. This contrasts with the strong effects that are often observed on a presynaptic neuron in the absence of its target (Campos et al., 1992; Sink and Whitington, 1991), and may reflect the existence of other targets of the BN in this region (Mukhopadhyay and Campos, 1995). However, the severe deficiency of the BN, in *glass*, GMR-*hid* or *so*^{mda} flies, had a drastic effect on the dendritic tree of the LNs. This demonstrates that the BN is required for proper morphogenesis of the LNs, and suggests that the BN is the main afferent connection to these clock cells. Interestingly, the BN is required also for the development of a serotonergic

arborization that contacts its ending in late second instar larvae (Mukhopadhyay and Campos, 1995). This contact suggests a serotonin-mediated modulation of BN-mediated light input to the larval brain clock. An inhibitory role of serotonergic afferents on retinal input to the mammalian suprachiasmatic nucleus has been well documented (Morin, 1999), and is described for some effects of light on insect clocks (Cymborowski, 1998).

Presynaptic nerve activity is often involved in the development or stability of postsynaptic elements (Cline, 2001). Our results point towards the involvement of some phototransduction-independent activity of the BN in the proper development of the dendritic arbor of clock cells. The disappearance of chaoptin expression in the BN at the beginning of metamorphosis correlates with a strong reduction of that arbor, which is also suggestive of a functional connection between the BO photoreceptors and the clock cells. The striking neuritic extension from the LNs that we observed in larvae expressing the KIR2.1 potassium channel in the BN has its counterpart in a small fraction of wild-type prepupae, consistent with the BN activity being altered at this developmental stage. Remodeling of dendritic arborizations during metamorphosis has been described for several subsets of larval neurons that persist into the adult stage (Tissot and Stocker, 2000).

The HB eyelet differentiates concomitantly with and projects to the adult LN_vs

Taken together, our anatomical and genetic data identify the adult LN_vs-contacting photoreceptors as the HB eyelet (Hofbauer and Buchner, 1989; Robinow and White, 1991; Yasuyama and Meinertzhagen, 1999). As expected, their projections run close to the surface of the medulla to reach the anterior part of this neuropil, and they are present in the so^1 mutant. In the wild type, the very extensive contact zone between these visual afferences and a PDF-expressing arborization closely matches the ventral extension of the accessory medulla, which was proposed as the target of visual inputs to the clock (Helfrich-Förster, 1997).

During metamorphosis, the absence of chaoptin-expressing visual afferences to the LNs may last over 30 hours. Cryptochrome may thus be the only light input pathway to the clock during this time window. Chaoptin-expressing fibers contact the LNs again from 45 hours APF, at about the same time when the l-LN_vs are first detected using *pdf-gal4* as a marker. In the adult, the HB eyelet neurons appear to express both histamine and acetylcholine (Hofbauer and Buchner, 1989; Yasuyama and Meinertzhagen, 1999). Whether both neurotransmitters are used for the light input to the adult LN_vs, and if so, whether they target the small and large LN_vs, or only one of the two groups, remains to be investigated.

Our observations are consistent with the report of three to six eyelet cells (Yasuyama and Meinertzhagen, 1999). The same report indicated that the eyelet expresses RH6 but not RH1, RH4 and RH5 rhodopsins. We too could not detect any anti-RH5 labeling, but weak *rh5* expression was detected in the HB photoreceptors with a *rh5-gal4* transgene, with most brains showing no *rh5* expression. As mentioned above, *rh5* and *rh6* expressions are mutually exclusive in the retinal R8 cells, and our data suggest that the same rule may hold in the BO. In the retina, *rh5* is expressed in only a minority of the R8 cells (Pichaud et al., 1999). Similarly, *rh5* could be expressed in only a minority of HB photoreceptors (and plausibly none in some eyelets, given the small number of cells). In any case, the low RH5 expression in the eyelet suggests that the relative contributions of RH5 and RH6 to circadian photoreception are different. These contributions could be tested by the analysis of circadian photoreception in specific rhodopsin mutants.

The possibility that the HB eyelet derives from the BO has been discussed in several studies. Despite differences in the number and position of cell bodies (Hofbauer and Buchner, 1989; Meinertzhagen and Hanson, 1993; Yasuyama and Meinertzhagen, 1999), and the 30 hours temporal gap between the disappearance of the BN and the detection of the eyelet (see above), recent results suggest that the eyelet cells may indeed be BO survivors (T. Edwards and I. A. Meinertzhagen, personal communication). This is in agreement with our finding that the BO and the eyelet appear to express the same phototransduction components. However, the presence of the HB eyelet in a few so^{mda} mutant adults, whereas the BN is never observed in larvae (Serikaku and O'Tousa, 1994), would rather support a BO-independent origin for the eyelet. Alternatively, so^{mda} BO/eyelet precursors could be able to project into the brain, and enter their final differentiation program during metamorphosis, without prior embryonic differentiation as BO photoreceptors.

The HB eyelet has been proposed to be a circadian photoreceptive organ (Hofbauer and Buchner, 1989; Yasuyama and Meinertzhagen, 1999). Our findings that its axonal projections directly contact the PDF-expressing arborization of the LN_vs in the accessory medulla strongly support this hypothesis. How might the eyelet contribute to clock responses to light? Adult $norpA^{p41}$; cry^b double mutants still entrain to LD cycles (Emery et al., 2000; Stanewsky et al., 1998), while gl^{60J} cry^b double mutants do not (Helfrich-Forster et al., 2001), suggesting the presence of *glass*-dependent, *norpA*- and *cry*-independent adult photoreceptors. Because the HB eyelet is absent in *glass* mutants, it appeared to be a candidate for such photoreceptors (Hall, 2000; Helfrich-Förster et al., 2001). Our finding that *norpA* is expressed in the eyelet strongly suggests that this structure actually participates to *norpA*-dependent circadian photoreception. PER-expressing dorsal neurons were recently shown to be missing in adult gl^{60J} brains, making them alternative candidates for *norpA*-independent circadian photoreceptors (Hall, 2000; Helfrich-Förster et al., 2001).

This work was supported by grants from CNRS (ATIPE 'Développement' and appel d'offres 'Biologie cellulaire') and Fondation pour la Recherche Médicale. S. M. is supported by the MENRT and F. R. by INSERM. We are grateful to the Bloomington *Drosophila* Stocks Center for the efficient mailing of many fly stocks; to A. Bergman for the GMR-*hid* strain; to J. R. Nambu for the UAS-*rpr* UAS-*hid* flies; to S. L. Zipursky for so^{mda}; to K. R. Rao for providing anti-PDF antiserum; to A. Hofbauer for the mAb 24B10 antibody; to R. D. Shortridge for the gift of the anti-NORPA antiserum and the *rh1-norpA* flies; to P. Salvaterra for the gift of the mAb 4B1 anti-ChAT antibody; to S. G. Britt for the gift of anti-RH5 and -RH6 antibodies; to F. Pichaud, P. Beaufils and C. Desplan for providing the various rhodopsin reporter lines and the *ro-tauZ* flies, and for sharing unpublished results; to F. Pichaud and U. Gaul for suggesting use of the *ro-tauZ* line to detect the eyelet in wild-type flies; to R. Baines for suggesting that we try the UAS-*Kir 2.1* flies and for giving them out; to S. Brown (CNRS, Gif/Yvette) and J. Salamero (Institut Curie, Paris) for generous assistance with confocal microscopes; to E. Chélot

for help with dissections; and to A. Lamouroux and C. Michard-Vanhée for their comments on the manuscript. J.-B. Coutelis and N. Capitaine contributed to this work during a summer stay in the laboratory.

REFERENCES

Baines, R. A., Uhler, J. P., Thompson, A., Sweeney, S. T. and Bate, M. (2001). Altered electrical properties in Drosophila neurons developing without synaptic transmission. *J. Neurosci.* **21**, 1523-1531.

Bergmann, A., Agapite, J., McCall, K. and Steller, H. (1998). The Drosophila gene hid is a direct molecular target of Ras-dependent survival signaling. *Cell* **95**, 331-341.

Blanchardon, E., Grima, B., Klarsfeld, A., Chélot, A., Hardin, P. E., Préat, T. and Rouyer, F. (2001). Defining the role of Drosophila lateral neurons in the control of circadian activity and eclosion rhythms by targeted genetic ablation and PERIOD protein overexpression. *Eur. J. Neurosci.* **13**, 871-888.

Bonini, N. M., Leiserson, W. M. and Benzer, S. (1993). The *eyes absent* gene: genetic control of cell survival and differentiation in the developing Drosophila eye. *Cell* **72**, 379-395.

Busto, M., Iyengar, B. and Campos, A. R. (1999). Genetic dissection of behavior: modulation of locomotion by light in the Drosophila melanogaster larva requires genetically distinct visual system functions. *J. Neurosci.* **19**, 3337-3344.

Campos, A. R., Fischbach, K. F. and Steller, H. (1992). Survival of photoreceptor neurons in the compound eye of Drosophila depends on connections with the optic ganglia. *Development* **114**, 355-366.

Campos, A. R., Lee, K. J. and Steller, H. (1995). Establishment of neuronal connectivity during development of the Drosophila larval visual system. *J. Neurobiol.* **28**, 313-329.

Cheyette, B. N., Green, P. J., Martin, K., Garren, H., Hartenstein, V. and Zipursky, S. L. (1994). The Drosophila sine oculis locus encodes a homeodomain-containing protein required for the development of the entire visual system. *Neuron* **12**, 977-996.

Chou, W. H., Hall, K. J., Wilson, D. B., Wideman, C. L., Townson, S. M., Chadwell, L. V. and Britt, S. G. (1996). Identification of a novel Drosophila opsin reveals specific patterning of the R7 and R8 photoreceptor cells. *Neuron* **17**, 1101-1115.

Cline, H. T. (2001). Dendritic arbor development and synaptogenesis. *Curr. Opin. Neurobiol.* **11**, 118-126.

Cymborowski, B. (1998). Serotonin modulates a photic response in circadian locomotor rhythmicity of adults of the blow fly *Calliphora vicina*. *Physiol. Entomol.* **23**, 25-32.

Dircksen, H., Zahnow, C. A., Gaus, G., Keller, R., Rao, K. R. and Riehm, J. P. (1987). The ultrastructure of nerve endings containing pigment-dispersing hormone (PDH) in crustacean sinus glands: identification by an antiserum against synthetic PDH. *Cell Tissue Res.* **250**, 377-387.

Emery, P., So, W. V., Kaneko, M., Hall, J. C. and Rosbash, M. (1998). CRY, a Drosophila clock and light-regulated cryptochrome, is a major contributor to circadian rhythm resetting and photosensitivity. *Cell* **95**, 669-679.

Emery, P., Stanewsky, R., Helfrich-Förster, C., Emery-Le, M., Hall, J. C. and Rosbash, M. (2000). Drosophila CRY is a deep brain circadian photoreceptor. *Neuron* **26**, 493-504.

Fujita, S. C., Zipursky, S. L., Benzer, S., Ferrus, A. and Shotwell, S. L. (1982). Monoclonal antibodies against the Drosophila nervous system. *Proc. Natl. Acad. Sci. USA* **79**, 7929-7933.

Green, P., Hartenstein, A. Y. and Hartenstein, V. (1993). The embryonic development of the Drosophila visual system. *Cell Tissue Res.* **273**, 583-598.

Hall, J. C. (2000). Cryptochromes: sensory reception, transduction, and clock functions subserving circadian systems. *Curr. Opin. Neurobiol.* **10**, 456-466.

Hardie, R. C., Raghu, P., Moore, S., Juusola, M., Baines, R. A. and Sweeney, S. T. (2001). Calcium influx via TRP channels is required to maintain PIP2 levels in Drosophila photoreceptors. *Neuron* **30**, 149-159.

Hassan, J., Busto, M., Iyengar, B. and Campos, A. R. (2000). Behavioral characterization and genetic analysis of the Drosophila melanogaster larval response to light as revealed by a novel individual assay. *Behav. Genet.* **30**, 59-69.

Hay, B. A., Wolff, T. and Rubin, G. M. (1994). Expression of baculovirus P35 prevents cell death in Drosophila. *Development* **120**, 2121-2129.

Helfrich-Förster, C. (1998). Robust circadian rhythmicity of Drosophila melanogaster requires the presence of lateral neurons: a brain-behavioral study of disconnected mutants. *J. Comp. Physiol. A* **182**, 435-453.

Helfrich-Förster, C. (1997). Development of pigment-dispersing hormone-immunoreactive neurons in the nervous system of Drosophila melanogaster. *J. Comp. Neurol.* **380**, 335-354.

Helfrich-Förster, C., Winter, C., Hofbauer, A., Hall, J. C. and Stanewsky, R. (2001). The circadian clock of fruit flies is blind after elimination of all known photoreceptors. *Neuron* **30**, 249-261.

Hofbauer, A. and Buchner, E. (1989). Does Drosophila have seven eyes? *Z Naturforsch [C]* **76**, 335-336.

Huber, A., Schulz, S., Bentrop, J., Groell, C., Wolfrum, U. and Paulsen, R. (1997). Molecular cloning of Drosophila Rh6 rhodopsin: the visual pigment of a subset of R8 photoreceptor cells. *FEBS Lett.* **406**, 6-10.

Kaneko, M., Helfrich-Förster, C. and Hall, J. C. (1997). Spatial and temporal expression of the period and timeless genes in the developing nervous system of drosophila: newly identified pacemaker candidates and novel features of clock gene product cycling. *J. Neurosci.* **17**, 6745-6760.

Kaneko, M., Hamblen, M. J. and Hall, J. C. (2000). Involvement of the period gene in developmental time-memory: effect of the perShort mutation on phase shifts induced by light pulses delivered to Drosophila larvae. *J. Biol. Rhythms* **15**, 13-30.

Kim, S., McKay, R. R., Miller, K. and Shortridge, R. D. (1995). Multiple subtypes of phospholipase C are encoded by the norpA gene of Drosophila melanogaster. *J. Biol. Chem.* **270**, 14376-14382.

Kitamoto, T. (2001). Conditional modification of behavior in Drosophila by targeted expression of a temperature-sensitive shibire allele in defined neurons. *J. Neurobiol.* **47**, 81-92.

Lee, T. and Luo, L. (1999). Mosaic analysis with a repressible neurotechnique cell marker for studies of gene function in neuronal morphogenesis. *Neuron* **22**, 451-461.

McKay, R. R., Chen, D. M., Miller, K., Kim, S., Stark, W. S. and Shortridge, R. D. (1995). Phospholipase C rescues visual defect in norpA mutant of Drosophila melanogaster. *J. Biol. Chem.* **270**, 13271-13276.

Meinertzhagen, I. A. and Hanson, T. E. (1993). The development of the optic lobe. In *The Development of* Drosophila melanogaster. Vol. II (ed. M. Bate and A. Martinez Arias), pp. 1363-1491. Cold Spring Harbor: Cold Spring Harbor Laboratory Press.

Morin, L. P. (1994). The circadian visual system. *Brain Res. Rev.* **19**, 102-127.

Morin, L. P. (1999). Serotonin and the regulation of mammalian circadian rhythmicity. *Ann. Med.* **31**, 12-33.

Moses, K., Ellis, M. C. and Rubin, G. M. (1989). The *glass* gene encodes a zinc-finger protein required by Drosophila photoreceptor cells. *Nature* **340**, 531-536.

Moses, K. and Rubin, G. M. (1991). *glass* encodes a site-specific DNA-binding protein that is regulated in response to positional signals in the developing Drosophila eye. *Genes Dev.* **5**, 583-593.

Mukhopadhyay, M. and Campos, A. R. (1995). The larval optic nerve is required for the development of an identified serotonergic arborization in Drosophila melanogaster. *Dev. Biol.* **169**, 629-643.

Papatsenko, D., Sheng, G. and Desplan, C. (1997). A new rhodopsin in R8 photoreceptors of Drosophila: evidence for coordinate expression with Rh3 in R7 cells. *Development* **124**, 1665-1673.

Papatsenko, D., Nazina, A. and Desplan, C. (2001). A conserved regulatory element present in all Drosophila rhodopsin genes mediates Pax6 functions and participates in the fine-tuning of cell-specific expression. *Mech. Dev.* **101**, 143-153.

Park, J. H., Helfrich-Förster, C., Lee, G., Liu, L., Rosbash, M. and Hall, J. C. (2000). Differential regulation of circadian pacemaker output by separate clock genes in Drosophila. *Proc. Natl. Acad. Sci. USA* **97**, 3608-3613.

Pearn, M. T., Randall, L. L., Shortridge, R. D., Burg, M. G. and Pak, W. L. (1996). Molecular, biochemical, and electrophysiological characterization of Drosophila norpA mutants. *J. Biol. Chem.* **271**, 4937-4945.

Pichaud, F. and Desplan, C. (2001). A new visualization approach for identifying mutations that affect differentiation and organization of the Drosophila ommatidia. *Development* **128**, 815-826.

Pichaud, F., Briscoe, A. and Desplan, C. (1999). Evolution of color vision. *Curr. Opin. Neurobiol.* **9**, 622-627.

Pignoni, F., Hu, B. R., Zavitz, K. H., Xiao, J. A., Garrity, P. A. and Zipursky, S. L. (1997). The eye-specification proteins so and eya form a complex and regulate multiple steps in Drosophila eye development. *Cell* **91**, 881-891.

Plautz, J. D., Kaneko, M., Hall, J. C. and Kay, S. A. (1997). Independent photoreceptive circadian clocks throughout Drosophila. *Science* **278**, 1632-1635.

Renn, S. C., Park, J. H., Rosbash, M., Hall, J. C. and Taghert, P. H. (1999). A pdf neuropeptide gene mutation and ablation of PDF neurons each cause severe abnormalities of behavioral circadian rhythms in Drosophila. *Cell* **99**, 791-802.

Robinow, S. and White, K. (1991). Characterization and spatial distribution of the ELAV protein during *Drosophila melanogaster* development. *J. Neurobiol.* **22**, 443-461.

Schmucker, D., Jackle, H. and Gaul, U. (1997). Genetic analysis of the larval optic nerve projection in Drosophila. *Development* **124**, 937-948.

Sehgal, A., Price, J. and Young, M. W. (1992). Ontogeny of a biological clock in Drosophila melanogaster. *Proc. Natl. Acad. Sci. USA* **89**, 1423-1427.

Serikaku, M. A. and O'Tousa, J. E. (1994). sine oculis is a homeobox gene required for Drosophila visual system development. *Genetics* **138**, 1137-1150.

Sink, H. and Whitington, P. M. (1991). Early ablation of target muscles modulates the arborisation pattern of an identified embryonic Drosophila motor axon. *Development* **113**, 701-707.

Stanewsky, R., Kaneko, M., Emery, P., Beretta, B., Wager-Smith, K., Kay, S. A., Rosbash, M. and Hall, J. C. (1998). The cryb mutation identifies cryptochrome as a circadian photoreceptor in Drosophila. *Cell* **95**, 681-692.

Tissot, M. and Stocker, R. F. (2000). Metamorphosis in drosophila and other insects: the fate of neurons throughout the stages. *Prog. Neurobiol.* **62**, 89-111.

Tix, S., Minden, J. S. and Technau, G. M. (1989). Pre-existing neuronal pathways in the developing optic lobes of *Drosophila*. *Development* **105**, 739-746.

Wheeler, D. A., Hamblen-Coyle, M. J., Dushay, M. S. and Hall, J. C. (1993). Behavior in light-dark cycles of Drosophila mutants that are arrhythmic, blind, or both. *J. Biol. Rhythms* **8**, 67-94.

Yang, Z., Emerson, M., Su, H. S. and Sehgal, A. (1998). Response of the timeless protein to light correlates with behavioral entrainment and suggests a nonvisual pathway for circadian photoreception. *Neuron* **21**, 215-223.

Yasuyama, K. and Meinertzhagen, I. A. (1999). Extraretinal photoreceptors at the compound Eye's posterior margin in Drosophila melanogaster. *J. Comp. Neurol.* **412**, 193-202.

Yasuyama, K., Kitamoto, T. and Salvaterra, P. M. (1995). Localization of choline acetyltransferase-expressing neurons in the larval visual system of Drosophila melanogaster. *Cell Tissue Res.* **282**, 193-202.

Zhou, L., Schnitzler, A., Agapite, J., Schwartz, L. M., Steller, H. and Nambu, J. R. (1997). Cooperative functions of the reaper and head involution defective genes in the programmed cell death of Drosophila central nervous system midline cells. *Proc. Natl. Acad. Sci. USA* **94**, 5131-5136.

Zhu, L., McKay, R. R. and Shortridge, R. D. (1993). Tissue-specific expression of phospholipase C encoded by the norpA gene of Drosophila melanogaster. *J. Biol. Chem.* **268**, 15994-16001.